LA-UR- 11-03423

Approved for public release; distribution is unlimited.

Title:	Spent Fuel Characterization using the Differential Die-Away Self-Interrogation Technique
Author(s):	Melissa A. Schear Howard O. Menlove Louise G. Evans Stephen J. Tobin Stephen Croft
Intended for:	52nd Annual Institute of Nuclear Materials Management Palm Desert, CA, U.S.A. 17-21 July, 2011

Los Alamos
NATIONAL LABORATORY
EST. 1943

Form 836 (7/06)

SPENT FUEL CHARACTERIZATION USING THE DIFFERENTIAL DIE-AWAY SELF-INTERROGATION TECHNIQUE

M. A. Schear, H. O. Menlove, S. J. Tobin, L.G. Evans, and S. Croft
Nuclear Nonproliferation Division, Los Alamos National Laboratory
Email: mschear@lanl.gov

ABSTRACT

This paper summarizes the development of the Differential Die-Away Self-Interrogation Technique (DDSI) as a non-destructive assay (NDA) method to measure the fissile mass present in 17x17 pressurized water reactor (PWR) spent fuel assemblies. The Monte Carlo N-Particle eXtended transport code, MCNPX [1], was used to create a library of 64 spent fuel assembly models [2] for simulations purposes within the modeled DDSI geometry, in order to study the detector response to assemblies of varying burnup (BU), initial enrichment (IE), and cooling time (CT). The comprehensive range of these parameters was intended to reflect the range of possible spent fuel assemblies encountered at various facilities worldwide, and the resulting isotopic complexity within those samples. The purpose of modeling is to relate the DDSI detector response to the given fissile mass. Based on this quantitative relation, fissile mass in spent fuel can then be measured experimentally. This paper outlines the DDSI detector configuration, and the determination of two viable ratios, the late gate doubles-to-singles (D/S) ratio and the late-to-early-gate doubles $(L/E)_D$ ratio, which both track with the fissile content of the assemblies. A ^{239}Pu-effective fissile mass concept was used as the basis for quantifying fissile mass, and relating such masses to the ratios. Both ratios were heavily dependent on BU, CT and IE of the assemblies and exhibited similar trends with the salient structure depending on IE. Multiplication within the assembly was used as a key intermediate parameter to develop a predictive model for effective mass values based on the ratios obtained from simulation. Using this model, there was a maximum of 6% deviation across the library between the true effective mass and the predicted effective mass based on the D/S ratio. This work is part of a larger effort sponsored by the Next Generation Safeguards Initiative (NGSI) to develop an integrated instrument, comprised of individual NDA techniques with complementary features, that is fully capable of determining Pu mass in spent fuel assemblies [3].

INTRODUCTION

The NDA of spent fuel to measure fissile isotopes is challenging since direct neutron and gamma signatures from those isotopes are masked by the high gamma-ray dose from fission products and the high neutron background from spontaneous fission and (α, n) reactions. In this paper, we propose the DDSI technique as a method to quantify the fissile content in spent fuel. The DDSI technique is similar to traditional differential die-away analysis, but it does not require a pulsed neutron generator or a pulsed beam accelerator, and it can, in certain cases, measure the mass of the spontaneous fission isotope in addition to the fissile mass [4, 5]. The method uses the spontaneous fission neutrons from ^{244}Cm within the assembly as the "pulsed" neutron source. The time correlated neutrons from the spontaneous fission and the subsequent induced fissions are analyzed as a function of time after the trigger event to determine the spontaneous fission rate and the induced fission rate in the sample. The time separation of the spontaneous fission and induced fission neutrons captured in the detector forms the basis of the technique, and the separate count rates obtained for each lead to the independent measurement of the spontaneous fission mass and

fissile mass. Spontaneous fission mass is determined by multiplicity analysis of the neutrons detected during an early gate (shown in Figure 1) which is opened soon after the initial triggering neutron is detected. Fissile mass is determined from the count rate acquired during the late gate. Induced fission occurs both with the fast neutrons at the time of spontaneous fission and also later in time with neutrons that have been moderated and reflected toward the assembly, i.e. thermal-neutron albedo.

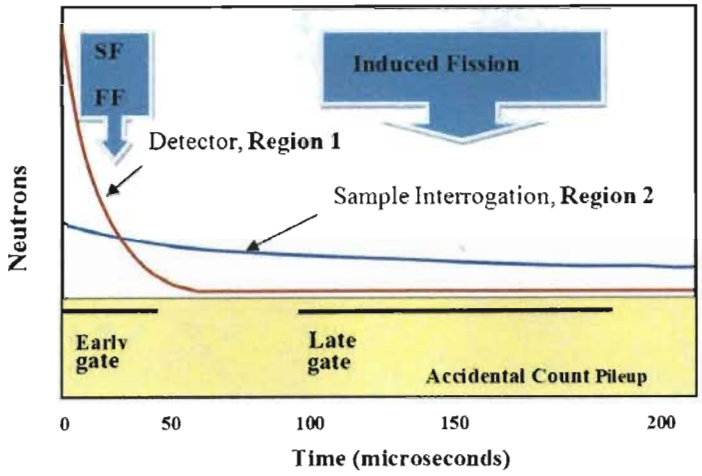

Figure 1: Conceptual neutron capture distributions in the DDSI detector from spontaneous fission (SF) and fast fission neutrons (FF) (fast die-away time) and thermal induced fission neutrons (slow die-away time) are used to select early and late gates.

MONTE CARLO SIMULATIONS

The DDSI Model

The time separation between the acquisition of spontaneous and thermal neutron induced fission counts is imposed by the dual region design of the DDSI detector model, as shown in Figure 2, which consists of a detector region with a high efficiency and short neutron die-away time and a sample interrogation region with a longer neutron die-away time. The die-away time of region 1, i.e. the detector region, is kept short by the use of a surrounding thermal-neutron cadmium filter which ensures that thermal neutrons that would otherwise extend the die-away time do not enter the detector region. Region 1 consists of 58 ^{3}He tubes, with 6 atm of pressure and a 40-cm active length, arranged in two concentric rows surrounding the centrally located spent fuel assembly. The ^{3}He tubes are embedded in a 7-cm thick annulus of polyethylene moderator, which is enveloped in a 1-mm thick cadmium liner to reduce the neutron die-away time. The optimized design has 13% detector efficiency to point ^{252}Cf source neutrons in air at the center of the instrument. Region 2 consists of a 1-cm thick polyethylene (CH_2) region surrounding the assembly to increase the induced fission rate within the assembly from reflected thermal neutrons. It is desirable to have a longer neutron die-away time in region 2 compared to region 1 so that there will be an imposed time lag between the detection of spontaneous and thermal induced fission events. For highly radioactive sample types, such as spent fuel, the high-Z reflector region serves a gamma shield for ^{3}He tubes. The concept has also been applied to spent fuel pins [6], as well as bulk Pu metal samples [7]. In the assembly library, burnup values are 15, 30, 45 and 60 GWd/tU. Initial enrichment values are 2, 3, 4, 5%, while cooling times are 1, 5, 20, and 80 years.

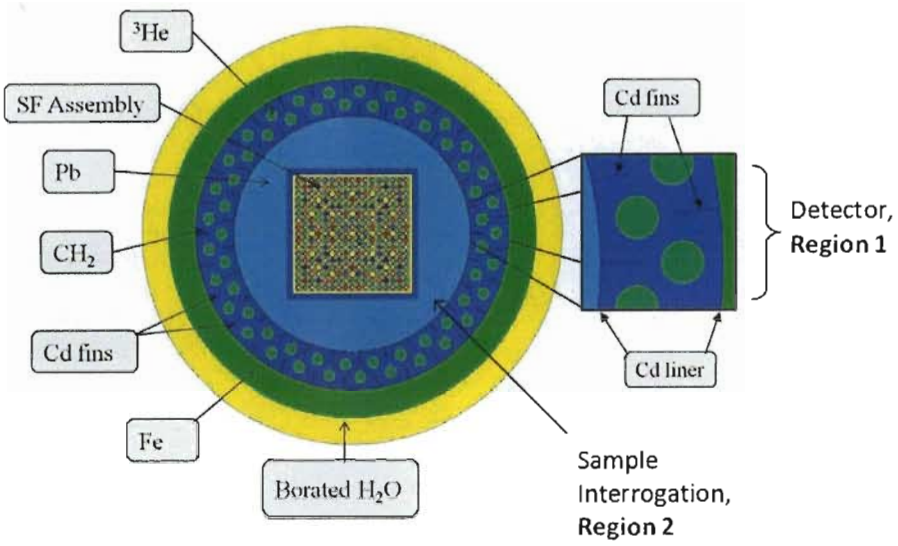

Figure 2: A horizontal cross-section of the DDSI detector configuration for MCNPX simulations is shown. An enlarged schematic of region 1 is shows the structure of the Cd fins. Region 1 is the exterior part of the instrument where neutrons are detected and region 2 is the interior region where reflected neutrons interrogate the assembly.

One of the primary purposes of this investigation is to provide DDSI-specific information to be used for possible integration with other NDA techniques for the purposes of the overall research effort. In 2009, the Next Generation Safeguards Initiative of the U.S. Department of Energy's National Nuclear Security Administration (NNSA) began a five-year effort to develop an integrated instrument fully capable of determining Pu mass in, and detecting diversion of pins from, spent commercial fuel assemblies. Following a rigorous, MCNPX-based evaluation of 14 individual measurement techniques (which includes DDSI) against a library of 64 spent fuel assemblies, efforts in 2012 will turn to the construction of one or more integrated systems comprised of the most promising techniques. This project brings together measurement and modeling experts from multiple U.S. national laboratories, several universities, and potentially one or more international partners.

Early and Late Gate Selection

Ideally, the early and late gates are chosen to maximize the spontaneous fission and induced fission counts, respectively, within each gate. Increasing the gate width increases these counts; however, there is an accidental pile-up continuum during both of these gates, as seen in Figure 1. In order to reduce the accidental pileup events in both gates, the gates should be made as short as possible. An optimum gate must be chosen to reduce the accidental pile-up effect while maximizing the spontaneous and induced fission counts. Previous work has expounded on the early and late gate width optimization for the geometry shown in Figure 2 [8]. Figure 3 shows the neutron capture time distribution of spontaneous and induced fission neutron events recorded in (a) a boron-loaded liquid scintillator detector (BC-523A) in the DDSI geometry (not shown) (b) the ^{3}He detector configuration, shown in Figure 2. The data was obtained via post processing PTRAC capture output file from the MCNPX code [9]. Referring to Figure 3a, the spontaneous fission (SF) distribution has a fast die-away, and after approximately 5 μs, there are no more SF captures following a given SF trigger event. Induced fission (IF) captures extend to later times, and the late gate is selected such that there are no SF captures occurring during that time. The liquid scintillator

detector provides good time separation between the SF and IF because of its short die-away time (1μs) compared to the sample region die-away (39μs). The ^{3}He-based detector provides a lesser degree of time separation, as seen in Figure 3b, where there is more of a "time smearing" between the two domains, i.e. for a large fraction of the time following a SF trigger event, there are both SF and IF captures, so the late gate is moved to later times where primarily IF captures occur, but unfortunately a large fraction of the IF response is not included. This time-smearing effect is due to the longer die-away of the ^{3}He bank (22 μs). The time gates for data evaluation for ^{3}He design were selected to be 0-4 μs for the early gate and 100-192 μs for the late gate.

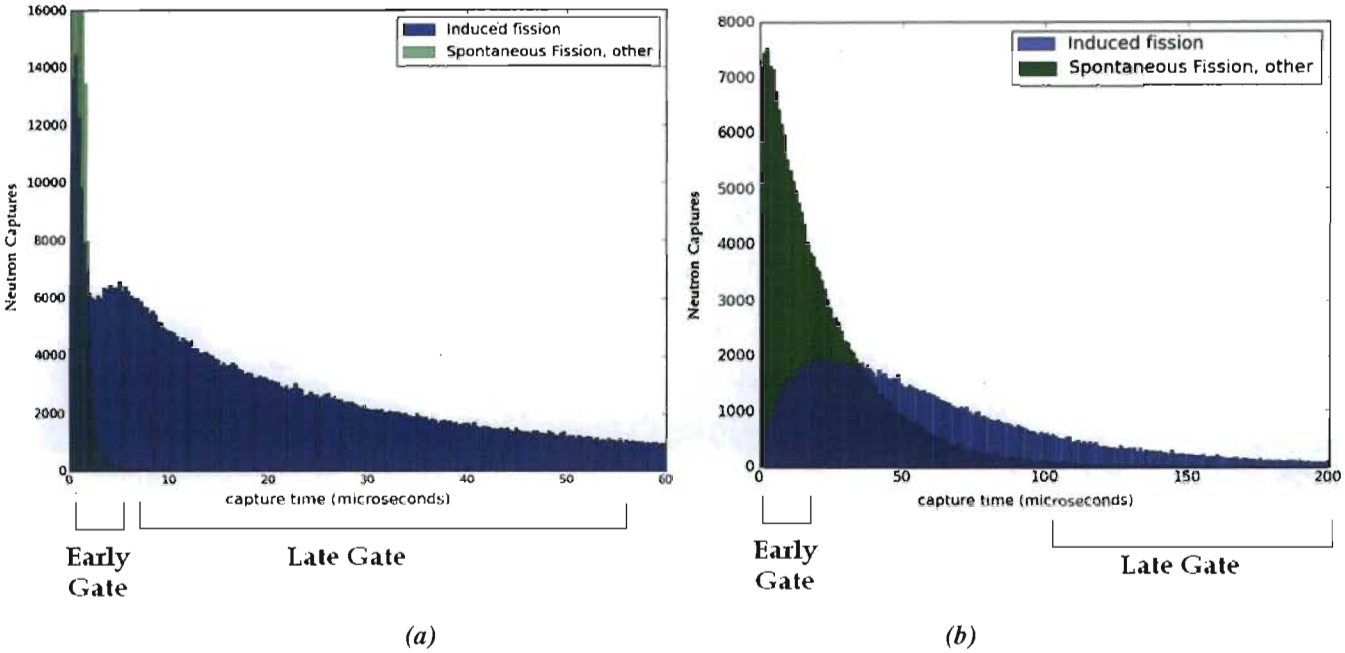

Figure 3: Simulated spontaneous and induced fission neutron capture time distributions in (a) boron-loaded liquid scintillator (b) bank of ^{3}He tubes. The spent fuel assembly measured was 30 GWd/tU, 5-year cooled, initially enriched to 3wt % ^{235}U.

For initial intents and purposes, the gate width selection is based solely on the PTRAC data for the remainder of this report. Note that the early gate of 0-4 μs chosen will also include the fast-neutron induced fission component, which cannot be circumvented with the current design, but our research objective is to assess the validity and performance of the DDSI technique with the current hardware limitations.

ANALYSIS

Effective Fissile Mass and DDSI ratios

The DDSI ratio is used infer effective fissile mass, as a first step in quantifying Pu mass. This relationship cannot be established via simple calibration for the complex spent fuel sample set, where three major fissile isotopes (^{235}U, ^{239}Pu, ^{241}Pu) all contribute toward the detected signal and the mass of the fissile isotopes vary with BU, IE and CT. Also, parasitic neutron absorbers, which diminish the detected neutron signal, also vary in a complex manner. Since the DDSI observed detector response in the late gate is due to the sum of the response from the three major fissile isotopes, we are measuring a combined mass. To this end, we have utilized a ^{239}Pu effective fissile

mass concept, captured by Equation 1, akin to the effective ^{240}Pu mass in passive multiplicity counting for the even plutonium isotopes [10], or the ^{239}Pu effective concept introduced previously for other non-spent fuel sample types [11]. The effective ^{239}Pu mass for induced fission weighs the relative contribution of the major fissile isotopes in the assembly toward the total effective mass. Specifically, the weighting coefficients, C_1 and C_2, give the relative contribution of the mass of each isotope toward the total effective mass, normalized to the contribution of ^{239}Pu. All the isotopes in Equation 1 are in mass units while the coefficients are dimensionless.

$$^{239}Pu_{eff} = C_1\,^{235}U + ^{239}Pu + C_2\,^{241}Pu \qquad \text{(Equation 1)}$$

The values of the coefficients in Equation 1, for each isotope, depend on the induced fission cross-section, σ_f, and subsequent neutron multiplicity distribution, as well as the detection probability of a fission neutron emitted by the isotope. MCNPX is capable of partitioning the relative contribution of each isotope toward the total detected signal. It is important to note that since the values of the C-coefficients depend not only on the neutronic properties of the isotope but also the neutron energy within in the fuel assembly. We expect that the greater the ^{239}Pu effective fissile mass present in the assembly, the greater the magnitude of the signal detected. We can therefore state that the relative contribution of an isotopic mass toward the total effective mass is akin to its relative contribution toward the total detected signal. By partitioning the detected counts to isolate counts coming from each of the major fissile isotopes, we can therefore calculate the magnitude of the C-coefficients. Although we cannot do this with experimental neutron counting, we have modified the MCNPX Particle Track Output (PTRAC) capture file capability to "label" the isotope from which the detected neutron originated [9]. The partition of the signal counts was done for the assemblies of major interest, and the average value of C_1 was found to be 0.45 with a variation of [-7%, 5%] and C_2 was 1.13 with a variation of [-3%, 2%] across the assembly library. Keep in mind that the C_1 and C_2 values from this approach are only dependent on the gross neutron counts seen in the detector from each isotope and not the coincident contribution in the detector. That is, it does not take the second fission moments of the isotopes into account (which are also energy dependent).

Referring to Figure 4a and 4b, we can now relate the late-to-early-gate ratio $(L/E)_D$ and the D/S ratio to the effective ^{239}Pu mass present in the 64 assemblies in the library. The effective mass values are obtained using equation 1 where the isotope mass values are known from the simulation input deck and the coefficient values are obtained also from the simulation results, as previously discussed.

Referring to Figure 4a and 4b, we can now relate the late-to-early-gate ratio $(L/E)_D$ and the D/S ratio to the effective ^{239}Pu mass present in the 64 assemblies in the library. The effective mass values are obtained using equation 1 where the isotope mass values are known from the simulation input deck and the coefficient values are obtained also from the simulation results, as previously discussed. The ratio values, also obtained from simulation, are normalized to the ratio from the assembly with the least fissile mass among the 64. Ideally, for a given ratio, there should be uniquely corresponding effective fissile mass. This is obviously not the case in Figure 4, where a given ratio may correspond to several fissile mass values depending on the initial enrichment of the assembly, i.e. the salient structure of the data is mainly dependent on the IE and BU of the assembly. The BU and CT dependence are shown in the plots. Note that both ratios, and hence the corresponding effective fissile masses, increase with decreasing burnup, increasing initial enrichment and decreasing cooling time, as expected.

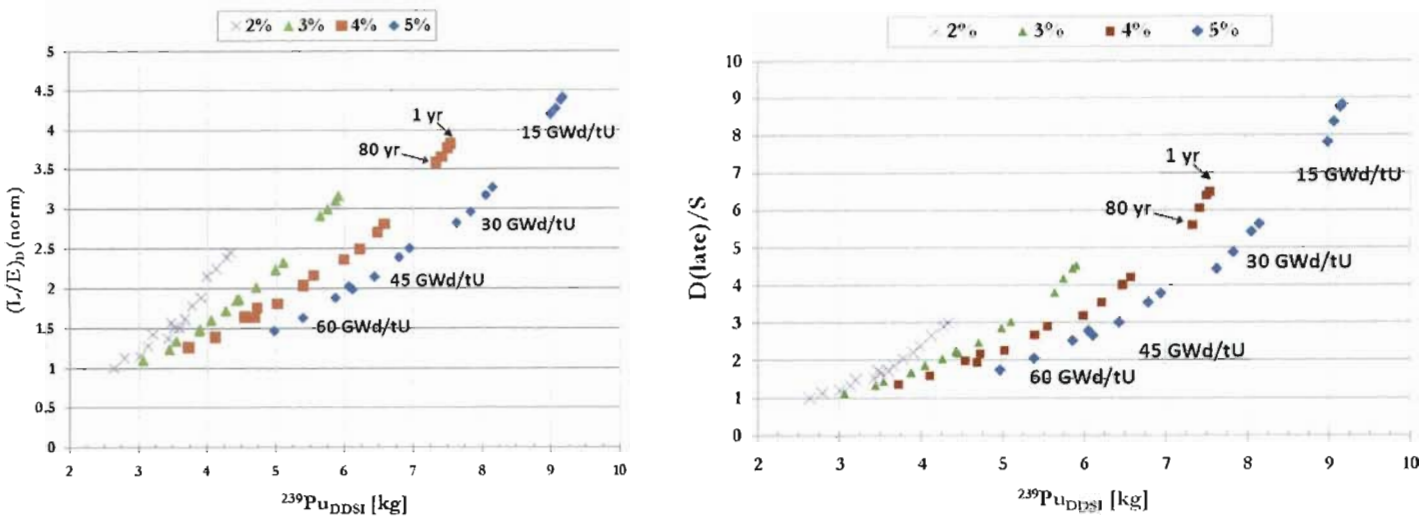

Figure 4: (a) Variation of the late-to-early-gate ratio and (b) D/S with effective ^{239}Pu mass for varying IE, BU, and CT for 64 assemblies in spent fuel library in borated water. Coefficients C_1 and C_2 are unique for each assembly.

Note that the normalized D/S ratio also shows a strong dependence on IE and BU, and spans a larger range than the $(L/E)_D$ ratio. For measurement purposes, we may consider the integration of the DDSI technique with a complementary neutron or photon technique capable of measuring initial enrichment of the spent fuel assembly. If the IE is known, then there will be a unique effective mass for a measured ratio.

Parametric Representation of Data Based on Assembly Multiplication

Figure 4 shows a clear dependence of the measured DDSI ratios on the ^{239}Pu effective mass present in the assembly, but due to the complicated structure of this dependence, one cannot readily obtain a ^{239}Pu effective mass value by simply fitting the data to obtain a functional fit, which can then be inverted to yield a mass value given a measured ratio. The goal is to derive a model, in essence, to infer an effective mass in an assembly from an experimentally-obtained ratio during an assay. A functional form relating either of the ratios to the effective mass values known to be in the assembly cannot be readily obtained, however, we may parameterize the data present in Figure 4 to relate both the effective mass and the DDSI ratio to an intermediate parameter for which we can more readily derive a functional fit heuristically. The DDSI ratios have a clear dependence on net multiplication in the assembly, as seen in Figure 5 for all 64 assemblies. The fit is a second order polynomial of the form seen in Equation 2a, and is based on the analytical derivation of D/S in Equation 2d based on definitions of singles and doubles shown in Equations 2b and 2c [12],

$$(D/S)=a\,(M)^2+b(M)+c \qquad \text{(Equation 2a)}$$

$$S=F\varepsilon M\nu_{s1}(1+\alpha) \qquad \text{(Equation 2b)}$$

$$D = \frac{F\varepsilon^2 f_d M^2}{2}\left[\nu_{s2} + \left(\frac{M-1}{\nu_{i1}-1}\right)\nu_{s1}(1+\alpha)\nu_{i2}\right] \quad \text{(Equation 2c)}$$

$$(D/S) = \beta M[1+(M-1)\,\kappa\,(1+\alpha)] \quad \text{(Equation 2d)}$$

$$M = \frac{d \cdot Pu239eff}{1+e \cdot Pu239eff} + 1 \quad \text{(Equation 3)}$$

where F is the spontaneous fission rate, (fission/s-g); ε is the neutron detection efficiency; M is the neutron leakage multiplication; α is the (α,n) to spontaneous fission neutron ratio; f_d is the doubles gate fraction, and f_t is the triples gate fraction. Note that from Equation 2d, the D/S ratio has a second order dependence on multiplication. The multiplication in this equation, however, is the leakage multiplication, which is proportional to the net multiplication in the assembly. We use 16 assemblies as the 'training data' used to establish a fit. These assemblies have varying BU and IE, but CT fixed at 5 years. The fit is then tested on the remaining 48 assemblies (varying CT) to determine the validity of the fit in predicting multiplication in the test data given a measured (D/S), as seen in Figure 5. This approach is called cross-validation, a technique used to estimate how accurately a predictive model, or fit, will perform for cases which were not used to establish the fit. The approach is to partition the 64 sample data set into two complementary subsets, performing the fit on one subset ("training data"), and assessing the validity of the established predictive model on the other subset ("test data"). Using this approach of training on 16 cases and testing on 48, the largest error across all 64 assemblies using the second order polynomial fit is 1.79%, which is for the least fissile assembly (2%, 60GWd/tU, and 80yr cooling time). Note that the predictive model performs well at predicting the multiplication in each assembly across the entire library, as shown in Figure 5. In general, the 80-yr cooling times exhibit more deviation of the fit from the data. However, these 80-yr CT cases may not be readily encountered when measuring fuel assemblies stored in an on-site pool, but may be encountered if measuring assemblies removed from dry storage casks in the future. For each IE group, there is a unique M for every measured (D/S). The purpose of establishing a reliable fit between the measured quantity (D/S) and multiplication is to then use the multiplication as an intermediate parameter, to which we can then relate the effective mass, using the "known M" approach [13]. So the process of determining the effective mass from a measured (D/S) effectively becomes a two-step process of (**1**) using the measured (D/S) to find net M (see figure 5) (**2**) using net M to find $^{239}Pu_{eff}$ using the functional relationship shown in Equation 3, which is an empirical fit used previously for fuel assemblies (see figure 6) [13].

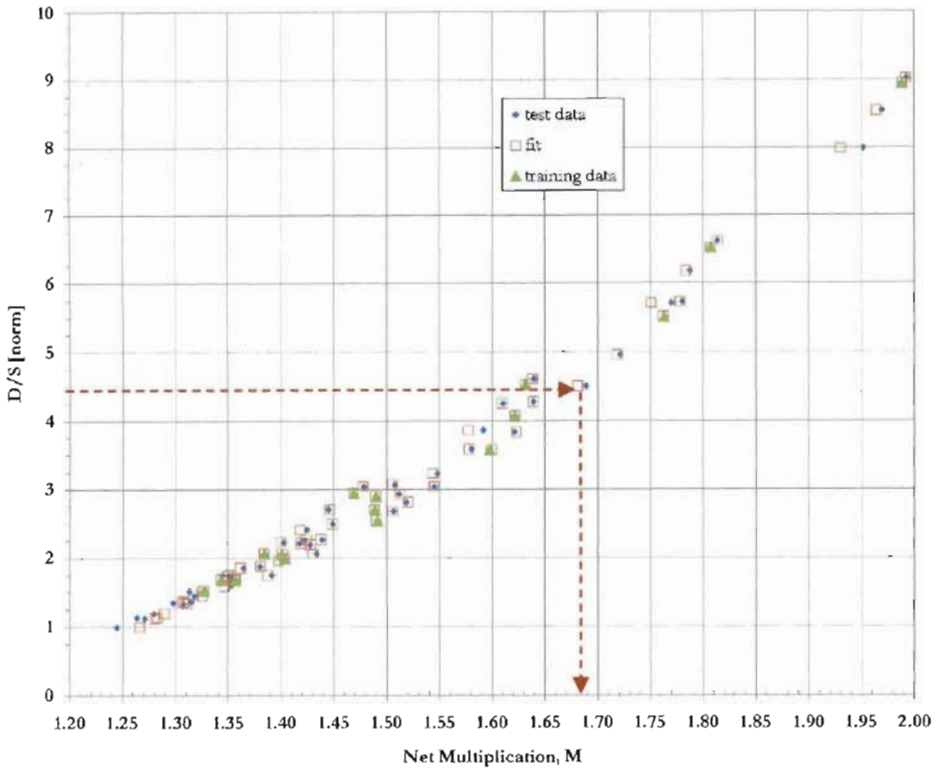

Figure 5: Actual D/S (norm) vs. Net M data and corresponding second order polynomial fit for all 64 cases

The purpose of this parameterization is to utilize commonly used safeguards analysis techniques: (a) the link between (D/S) and multiplication and (b) the link between multiplication and effective mass, in order to better understand the structure of the D/S vs. $^{239}Pu_{eff}$ function. For a given assembly type, each initial enrichment has slightly different **d** and **e** values, as shown in Fig 6. The inset plot on the bottom right corner in Figure 6 shows the grouping of the same data based on initial enrichment to emphasize this dependence. These parameter values are similar in magnitude to those found in previous publications [13]. Figure 6 shows step two of the process, where net M is used to obtain a ^{239}Pu effective mass using a predictive model based on equation 3. For the least fissile assembly, the deviation between the predicted value and the actual value is 5.6% which is the highest percentage error in the entire library. Figure 7 shows the deviation between the fit and the actual data for the DDSI ratio and $^{239}Pu_{eff}$ mass relation by collapsing the parameterization. Note that this predictive model performs well given the fact that we are only training our fit on one quarter (16/64) of our data.

CONCLUSIONS

This report has established the viability of using the DDSI technique for PWR spent fuel verification purposes. In this preliminary study, this has been done purely by modeling and simulation to obtain the response to a wide range of spent fuel assemblies. Simulations were performed for borated water as the surrounding media. We have established two DDSI measured ratios, D/S and $(L/E)_D$ which undoubtedly track the fissile content in the assemblies. These ratios show a large discrimination ratio across the spent fuel library samples, more so than the PNAR technique. The $(L/E)_D$ has the advantage of canceling out the source strength of the spontaneous fission driving term, as well as the detection efficiency. These ratios were related to the known effective mass of the assembly to investigate the correlation of these quantities. A preliminary parametric approach has been proposed where a measured DDSI ratio can be used to calculate the effective mass quantity using empirical multiplication relations as an intermediate step. Predicted

effective mass values have been obtained using a two-step predictive model, with mass deviations less than 6% across the entire library.

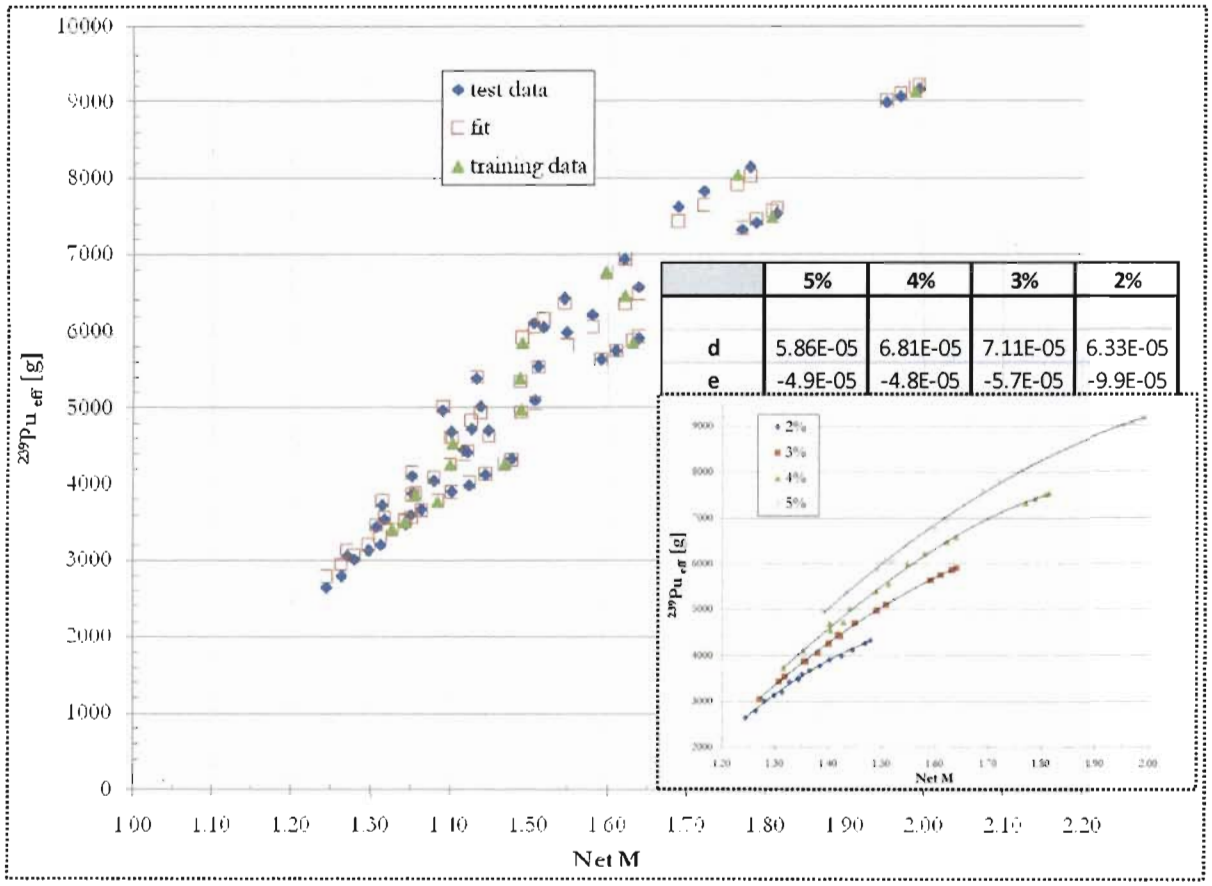

Figure 6: Actual $^{239}Pu_{eff}$ vs. net M data and corresponding fit for all 64 cases

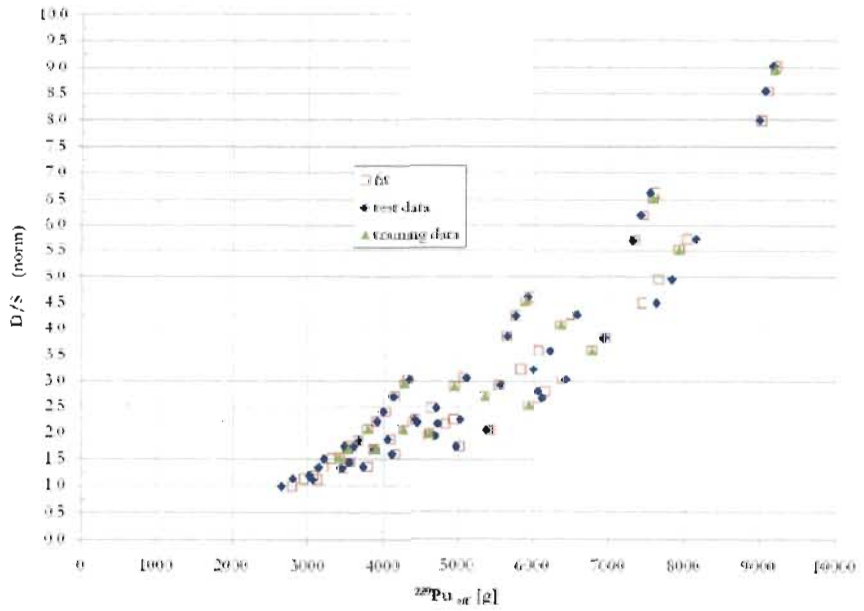

Figure 7: Predictive model fit for DDSI ratio vs. effective mass values.

ACKNOWLEDGMENTS

The authors would like to acknowledge the support of the Next Generation Safeguards Initiative (NGSI), Office of Nonproliferation and International Security (NIS), National Nuclear Security Administration (NNSA).

REFERENCES

1. J. F. Pelowitz (Editor), "MCNPXTM USER'S MANUAL Version 2.5.0," Los Alamos National Laboratory report LA-CP-05-0369 (2005).
2. M.L. Fensin, S.J. Tobin, N.P. Sandoval, M.T. Swinhoe, S.J. Thompson, "A Monte Carlo linked Depletion Spent Fuel Library for Assessing Varied Nondestructive Assay Techniques for Nuclear Safeguards," Advances in Nuclear Fuel Management IV (ANFM), Hilton Head Island, South Carolina, USA, April 12-15, 2009.
3. Kevin D. Veal, Stephen A. LaMontagne, Stephen J. Tobin, L. Eric Smith, "*NGSI Program to Investigate Techniques for the Direct Measurement of Plutonium in Spent LWR Fuels by Non-destructive Assay*," Institute of Nuclear Materials Management 51st Annual Meeting, Baltimore, MD (July 11-16, 2010).
4. H. O. Menlove, S. H. Menlove, and S. J. Tobin, "Fissile and Fertile Nuclear Material Measurements Using a New Differential Die-Away Self-Interrogation Technique", Nuclear Instruments and Methods in Physics Research A 602 588-593 (2009).
5. H.O. Menlove, S.H. Menlove, S.J. Tobin, "Verification of Plutonium content in Spent Fuel Assemblies Using Neutron Self-Interrogation," LA-UR-09-03715, Institute of Nuclear Materials Management 50th Annual Meeting, Tucson, AZ (July 12-16, 2009).
6. M. A. Schear, H.O. Menlove, S.J. Tobin, S. Y. Lee, L. G. Evans, "Fissile Isotope Discrimination using Differential Die-Away Self-interrogation Technique on a Single Pin Geometry," LA-UR 10-00092, American Nuclear Society 2010 Annual Meeting, San Diego, CA (June 13-18, 2010)
7. H. O. Menlove, M. A. Schear, M. T. Swinhoe, M. M. Bourne "Neutron Differential Die-away Self-Interrogation (DDSI) for the verification of Plutonium," Los Alamos National Laboratory report LA-CP-10-01553 (2010).
8. L.G. Evans, S.J. Tobin, S. Croft and M.A. Schear, "Gate Width Optimization for Passive Neutron Albedo Reactivity (PNAR) applied to the Non-Destructive Assay of Spent Nuclear Fuel", Published in Transactions of the American Nuclear Society (ANS) Annual Meeting (2010), San Diego, CA, USA.
9. Louise Evans, M.A. Schear, John Hendricks, M.T. Swinhoe, Stephen J. Tobin, Stephen Croft; "A New MCNPX PTRAC Coincidence Capture File Capability: A Tool for Neutron Detector Design," Waste Management Symposia, Phoenix, AZ; 2011
10. D.T. Reilly, "Passive Nondestructive Assay of Nuclear Materials," Office of Nuclear Regulatory Research, NUREG/CR-5550, Los Alamos National Laboratory Document LA-UR-90-732 (1990).
11. J. E. Stewart et al., "Defining an Effective Plutonium Mass for Induced Fission (IF)," in "Safeguards and Security Progress Report," compiled by D. B. Smith and G. R. Jaramillo, Los Alamos National Laboratory report LA-11356-PR, pp.18-21 (1987).
12. N. Ensslin, W. C. Harker, M. S. Krick, D. G. Langner, M. M. Pickrell, J. E. Stewart, "Application Guide to Neutron Multiplicity Counting," Los Alamos National Laboratory report LA-13422-M (1998).
13. H. O. Menlove, Zhu, et al, "The Analyses of Neutron Coincidence Data to Verify Both Spontaneous-Fission and Fissionable Isotopes" , (1989)